AIAA-99-1521

SIMULATION OF DEPLOYMENT DYNAMICS OF INFLATABLE STRUCTURES

Moktar Salama*, C. P. Kuo**, and Michael Lou*
Jet Propulsion Laboratory,
California Institute of Technology,
Pasadena, CA. 91109

Abstract

Analytical simulation of the inflation process of inflatable structures is key to assessing their robust deployment in **space environment.** This paper develops a simplified inflation model that allows description of the gas flow, pressure variation, and resulting large deformation throughout domains of the inflatable structure. Three different **packaging** /deployment schemes (Z-folding, rollout, and extrusion) are selected for illustration, and two nonlinear dynamic software (ADAMS, and LS-DYNA3D) are chosen for model implementation. The inflation model is not limited to prismatic one-dimensional components, and can be applied to inflatable shapes with complex configurations.

Simulation results are presented, which provide insight into the deployment of three examples of cylindrical tubes, initially stowed according to each of the above schemes. As a simple validation of the numerical simulation, a laboratory test was conducted on the Z-folded configuration. Good agreement in the overall inflation dynamics is observed.

1. Introduction

Several NASA space missions are being planned which consider the use of lightweight inflatable structures for components such as booms, sun-shades, solar concentrators, solar sails, and antennas for nearly all aspects of Earth and space missions. As a prelude to these missions, the IN-STEP Inflatable Antenna Experiment (IAE) was deployed from the space shuttle Endeavor in May 1996 to demonstrate the reliability of the inflatable technology for a large 14-meter antenna structure in a realistic space environment [1].

One of the urgent technology issues revealed by the brief 80-minute IAE flight experiment was the need to better understand the dynamics of deploying inflatable structures in space, and how the inflation process is influenced by the deployment scheme. This includes the initial packaging, and subsequent release and inflation mechanism. Depending on the deployment scheme, large inflatable structures can be extremely flexible to the point of instability – especially during the early stages of inflation. Rigidization can begin only after final deployment is achieved. Testing the deployment of a large inflatable in Earth environment in presence of gravity and air is of limited value for inferring their deployment behavior in space. Therefore, analytical models for simulating and predicting the dynamics of the inflation process are essential tools for understanding their deployment behavior in space environment, and for guiding and improving future packaging and deployment concepts.

---

* Associate Fellow, AIAA
** Senior Member, AIAA

To this end, this paper explores a modeling approach which allows simulation of the deployment process for simple prismatic inflatable configurations: from the initial stowed state – to full deployment. Of interest here, is a description of all states of inflation as a function of time. Knowledge of all states of inflation is essential for subsequent assessment of conditions of stability and controllability of the deployment process.

2. Deployment Concepts

Deployment schemes that have been proposed for inflatable structures may be classified dynamically as unrestricted free deployment, and controlled or guided deployment. This classification is closely related to details of the initial packaging, and the mechanisms used during inflation to control the release of the inflated and yet-to-be-inflated segments of the structure.

In the unrestricted deployment, inflated or partially inflated segments of the structure are not restrained from moving freely in space once released. In the process, their inertia could drag along other un-inflated segments, thereby giving rise to the deployment of components with undesirably high degree of flexibility. As a result, the system may become unstable prior to achieving full inflation. In controlled deployment, however, only inflated segments of the structure are allowed to deploy in space. Since fully inflated segments have much higher stiffness than partially inflated segments, systems with controlled deployment will tend to be much more stable dynamically.

The Z-folded packaging of tubes and lenticular membranes used in the IAE experiment is an example of unrestricted deployment. On the other hand, the mandrel-guided extrusion scheme - once proposed for inflation of cylindrical tubes for the Next Generation Space Telescope (NGST) - is an example of controlled deployment. This type of deployment scheme, however, can be used only for inflatables having prismatic shapes such as one-dimensional tubes, and is not applicable for other arbitrary shapes such as a torus or components of lenticular forms. Another example of controlled deployment has been used for the Inflatable Space Synthetic Aperture Radar [2], in which the inflatable structure is initially packaged by rolling. This scheme is perhaps the most common of the three concepts cited here. Depending on the configuration, rolling can be in a single or multiple directions. In addition, passive control of deployment can be introduced, typically in the form of built-in resistive force elements such as coil springs or surface-mounted Velcro strips.

In the following, we develop dynamic models for simulating the three deployment concepts above for inflatable prismatic cylindrical tubes.

3. Inflation Model

The forces that activate the deployment of inflatable thin shell structures are dominated by interactions between the flow of the inflating gas and the flexible shell that contains it. Other forces may be influential to various degrees, depending upon details of the packaging and release scheme under consideration. An example of the later is the restoring spring or surface contact forces in the rollout deployment.

We employ a gas flow–structure interaction model, which is suitable for use with all of the deployment concepts discussed above. In this model, the change in deformed inflatable volume $\Delta V_v(t)$ at time t is calculated over a small increment of time as a function of the instantaneous pressure, volume, and stress (or deformed) state of the shell material. Before inflation, the membrane shell is typically wrinkled and its effective elasticity modulus is extremely low. For the most part of the inflation process, the shell structure experiences large deformations while carrying very low stresses. A constitutive material model that is consistent with wrinkled membrane shell behavior is qualitatively illustrated by the schematic in Figure (1), where the effective modulus $E_{\max}$ (e.g. 2.6E+7 psi for a composite) is normalized at a unit fully inflated volume, V. A similar behavior was also evident from tests carried out on wrinkled membrane [3].

In addition to calculating the change in deformed volume, the internal pressure is also updated at each time increment as the inflation gas flows throughout the cavity. To simplify the interaction model between the membrane shell and the gas flow, we assume that the inflatable component is discretized internally into smaller compartments separated by artificial orifices. The inflation gas then flows between each pair of compartments, m and n, across the separating orifice whose area is A_{mn}. It is convenient to place the orifices at initial fold lines (if there is any), and to allow

their areas to vary with the local cross sectional area of the inflatable cavity. With this simplification, the internal pressure and volume of each compartment is taken to be spatially constant within a given compartment, but varies from one compartment to the next as inflation of the entire cavity progresses.

Consider an ideal gas flowing between two compartments m and n, across orifice A_{mn}. Depending on the ratio of pressures downstream and upstream from the orifice, the gas flow may be sonic or subsonic. For subsonic flow, the rate of flow dm_{mn} of mass of gas across the orifice can be approximated by one-dimensional quasi-steady flow [4], here expressed by:

$$dm_{mn}/dt = kA_{mn}P_d[(1/GT)(2\gamma/(\gamma-1)) \times (P_o/P_d)^{(\gamma-1)/\gamma}((P_u/P_d)^{(\gamma-1)/\gamma}-1)]^{1/2} \quad (1)$$

where: P_o, P_u, P_d are respectively the initial pressure, upstream pressure, and downstream pressure, γ = specific heat ratio, G = gas constant, T = gas temperature, and k = orifice coefficient [5].

Similarly, when the flow is sonic:

$$dm_{mn}/dt = kA_{mn}P_d[(1/GT)(2\gamma/(\gamma+1))^{((\gamma+1)/(\gamma-1))} \times (P_u/P_d)^{(\gamma+1)/\gamma}]^{1/2} \quad (2)$$

Depending on the type and direction of flow, either of the nonlinear Equations (1) or (2), can be integrated numerically for each pair of compartments m and n to calculate the mass of gas $\Delta m(t)$ transferred between them at each discrete time t in the simulation. Assuming constant density, the corresponding change in volume of each compartment, say compartment m, is computed as $(\Delta V_f(t))_m$. Other volumetric changes, here collectively referred to as $(\Delta V_v(t))_m$, arise from deformation of the membrane shell itself due to elasticity of the skin, or due to contact forces between the inflated surfaces, or any other source of deformation. The total change in volume of compartment m is simply the sum of all aforementioned effects:

$$\Delta V_m(t) = (\Delta V_f(t) + \Delta V_v(t))_m \quad (3)$$

The corresponding updated pressure is then found for a typical compartment from:

$$P_m(t) = P_o[V_o/(V_o - \Delta V_m(t))]^{\gamma} \quad (4)$$

For a given distribution of pressure $P_m(t)$ in discrete compartments of the inflatable component, one can propagate computation of the deformations dynamically to the next time step in the simulation. The same simplified gas flow model above was previously utilized in simulating attenuation in the airbag impact dynamics [6]. Other applications used similar concepts [7].

4. Numerical Simulations

In this section we present results of simulating the inflation of a cylindrical tube initially stowed in three different configurations. Two different nonlinear dynamics software were selected for model implementation: LS-DYNA3D [8] and ADAMS [9]. Both of these are commercially available nonlinear, large deformation, dynamic analysis software tools, but each has different computational primitives and environment.

i. Deployment of Z-Folded Tube

Consider the inflation of a cylindrical tube (diameter = 7 cm, length = 20 cm, .0125 cm thick, E =18E+10 N/m^2), initially folded flat into two overlaying segments. The gas inflation model described in the previous section is similar to the Simple_Airbag_Model in [8]. A finite element model of the tube in its folded state was constructed in a free-free condition as shown in the lower left corner of Figure (2). Over 900-shell elements capable of membrane and bending behavior were used. The folded tube was divided into two compartments separated at the fold line. The inflation gas is introduced mathematically into the first compartment in the form of mass flow rate as function of time. The two compartments are allowed to vent to each other mathematically across an orifice, whose area is proportional to the cross sectional area at the fold. Initially, the orifice area A_{mn} = 0, but as inflation progresses A_{mn} increases gradually until it becomes equal to the entire cross section.

Contact between all surfaces of the tube is maintained and checked during inflation using the Single_Surface_Contact algorithm. In this algorithm, the normal distances between nearest pairs of nodes are checked against a predetermined penetration tolerance. Account is taken of the shell thickness, and whether penetration is approaching from the negative or positive side. If penetration is detected at a pair of nodes, a pair of equal and opposite nodal forces is applied proportional to the penetration distance and surface stiffness k_i, approximated by $k_i = (0.1 * K_i A_i^2 / V_i)$, where K_i, A_i, V_i, are the bulk modulus, area and volume of the element containing the contacting segment. At nodes in contact, we also apply contact viscous damping (~10%), and Coulomb friction, having static and dynamic coefficients equal to .05 and .08, respectively.

The results in Figure (2), show that the gas flow allowed relatively slow pressure build-up into the first compartment, along with a gradual opening of the initially constricted cross section at the fold line (artificial orifice). As constriction of the fold eroded, the pressure in the second compartment rose to equal the pressure in the first compartment, immediately after the second fold snapped open. The maximum pressure differential between the two folds was about $280 N/m^2$. For the two-compartment configuration considered, we note nearly 20% time lag in pressurization between the two folds (approximately 1.6 seconds out of 8.0 seconds). This lag is dependent upon many parameters, including the shell model, surface contact model, and orifice area and its variation with time. In a multiple-fold configuration, the pressurization lag between the first and last fold is expected to increase with the number of folds. The implication here is that multiple Z-fold configurations tend to have larger percent of the tube length free to deploy while not fully pressurized. This leads to opportunities for dynamic instability, which can be excited by discontinuity in the contact forces. Just before the opening of each fold, the contact forces tend to reach their maximum, then become zero once the fold opens.

ii. Rollout Deployment

The circular tube under consideration is 5.6 cm diameter, 20 cm long, and is made of .0125 cm thick fabric material. The material properties are assumed as in the previous example. Initially, the tube is rolled in the form of an Archimedean linear spiral shape governed by $r = a\theta$, as in the configuration shown in the lower left corner of Figure (3). The finite element model of this configuration is free-free and consists of 392 shell elements connecting 364 nodes. Here again, the inflation model of Section 3 is implemented by subdividing the tube into five compartments along the rolling direction, separated by artificial orifices. Two of the five compartments are in the straight section of the tube, and the remaining ones are in the spiral section. Successive pairs of compartments are allowed to vent to each other across the shared artificial orifice. As in the previous example, the area of each orifice is function of the local cross sectional area. Initially, all orifice areas are nearly zero, but they increase sequentially and gradually as inflation progresses from one end of the tube to the other.

In terms of contact forces, no scheme of deployment is more dominated by continuity of forces between contacting surfaces than in rollout deployment. In rollout deployment, once the straight part of the tube is inflated, contact surface forces will remain at their peak while marching spatially along the rollout path until complete deployment. This is true, so long as the inflation pressure is monotonically maintained. The sequence of deployment and pressure build-up as gas flows from the straight end to the spiral part, is shown in Figure (3). The time at which each of the picture frames was taken from the animation corresponds approximately to the time location on the figure. For example, the last picture shown is recorded at about 3.8 seconds when the tube was nearly cylindrical, but not completely inflated. Further pressure increase to about 1800 N/m^2 was accompanied by elastic stretching of the membrane. Maximum pressure differential of about 150 N/m^2 is observed between the two ends of the tube. Unlike the Z-fold concept, the differential pressure between ends of a rolled tube is expected to remain the same regardless of the length of the tube. Furthermore, the stability of deployment of rolled tubes is maintained, not only by the restoring forces in the spiral, but also by the relatively smooth variation of the rollout forces between surfaces in contact. In the present results, resistive forces were not modeled but will be included in future work.

iii. Extrusion Deployment

Simulation of deployment of a cylindrical tube by extrusion (as in mandrel-guided inflation) is performed here within the framework of ADAMS software. Although primitives in ADAMS are best suited for simulating rigid body dynamics, it provides the ability to model flexible bodies - mostly as functional representation of forces.

Consider the inflation of a tube with diameter = 10 cm, length = 30 cm, thickness 0.01 cm. In this case, a single compartment one-dimensional flexible model is constructed, in which the state variable is the deployed position $z(t)$ of the closed end of the tube relative to the fixed mandrel. Initially, $z(0) = 0$. Then, the pressurization gas is introduced into the mandrel-side of the tube through an orifice connection to an inflation canister. At a typical instant of time the inflation gas creates internal pressure $P_m(t)$ in the tube, the magnitude of which is governed by Equations (1) to (4) of Section 3. The pressure forces $P_m(t)$ are simulated in ADAMS software along with other forces such as: forces due to tube's longitudinal stiffness $= 2\pi r t_o E^* z / L$, time dependent mass of inflated tube, and damping forces proportional to the velocity of inflation. The modulus used in the stiffness expression is that of the one-dimensional constitutive relationship of wrinkled membrane in Figure (1).

The results of simulation are shown in Figure (4). As in previous cases, the pressure internal to the tube is shown as function of time. Here, a small leak (2 mm^2) is assumed to exist between $t = 1.75$ and 2.0 seconds. Leakage is implemented by venting gas from the compartment in question to the outside across a 2 mm^2 orifice area. Four frames are selected from the animation at different time instances and are superimposed on the pressure curve in Figure (4). Full inflation is achieved in a highly stable fashion after approximately four seconds.

5. Validation Experiment

As a simple validation of the numerical simulation, a laboratory test was conducted using the configuration of Section 4-i, in which the tube is initially folded flat into two overlapping segments. The same approximate dimensions and material properties apply here. Inflation of the tube was provided by a pneumatic air pump fitted with a pressure regulator and flow meter to measure and control the air flow into the tube. The pressure in each of the folds was monitored by separate pressure gages attached to 1.5 mm silicone tubing inserted half way inside each fold. A high-resolution digital video camera was used for optical imaging of the inflation experiment. The images were subsequently captured frame-by-frame into a personal computer using ATI-multimedia software for further analysis and data reduction.

In Figure (5), the test results are presented in a form analogous to Figure (2). However, before comparison is made, we first note the differences between conditions of the test and analysis. Simplicity of the test setup did not allow inflation of the tube with the same speed of air flow as in the analysis. On the other hand, slowing down the inflation rate in the analysis was not considered because it increases the calculation time from minutes to days. Furthermore, both gravity and the internal silicone tubing inserted in the folds to monitor the pressure were not modeled in the analysis. So, comparison between Figures (2) and (5) can only be made qualitatively, with test time replaced by imaging frame. Despite these discrepancies, there is good agreement between the pressurization curves in the test and simulation - not only in the variation of pressure in each fold with time - but also in the magnitude of differential pressure between folds. This is also evident from a qualitative comparison of the degree of inflation indicated by images from the test and from analysis. The kink in the upper fold of the test images, Figure (5), is due to the additional mass and stiffness of the silicone tube inserted in the upper fold to monitor the pressure.

Considering the above remarks, we conclude that the modeling and analysis approach discussed herein is capable of capturing the overall dynamics of inflation relatively well, in spite of the idealizations introduced. Implementation of the inflation model in the flexible body LS-DYNA3D software is more natural than in the mostly rigid body ADAMS software.

6. Conclusions

The main objective of this paper was to explore the use of analysis simulation as a tool for verifying the dynamic behavior of the deployment

process of inflatable structures in space. This is desirable since experimental ground verification of these highly flexible nonlinear structures is often not possible. For this purpose, a unified inflation model was proposed for simulation of deployment on two different dynamics software that lie at two extremes: ADAMS software for rigid body dynamics, and LS-DYNA3D for flexible body dynamics. Naturally, the later software is much more suited for inflation analysis. The model allows for the spatial variation of pressure during inflation by introducing artificial compartmentalization in the inflatable cavity. If this idealization is not employed, the pressure will be invariant inside the entire inflatable cavity, and the resulting inflation sequence will be physically incorrect.

For simplicity, the three examples selected represented different schemes for inflating prismatic structural components, such as tubes. However, the inflation model is not limited to prismatic components, and can be applied to inflatable shapes with complex configurations.

In spite of the discrepancies noted between the analysis and test conditions and the idealizations implied by the model, the analysis simulations captured the overall dynamics of deployment relatively well.

In a future assessment of the detailed design of a given inflatable concept, we envision that the test configuration (including gravity) be first simulated in details. The purpose of this first phase of simulation would be to tune the analysis parameters to best match the test results. Once this phase is completed, deployment simulation of the space environment and configuration could be made with confidence.

7. Acknowledgements

This research was performed at the Jet Propulsion Laboratory, California Institute of Technology, under contract with the National Aeronautics and Space Administration. Funding was provided by JPL Director's Research and Development Fund. We gratefully acknowledge the help of J.J. Wu, JPL, in setup of experiment, and J. McKinney, of Virtual Engineer, for advising on use of DYNA3D.

8. References

[1]. Freeland, R.E., and Veal, G.,R., "Significance of the Inflatable Antenna Experiment Technology", proceedings of the 39th AIAA/ASME/ASCE/ AHS/ASC Structures, Structural Dynamics, and Materials Conference, Long Beach, CA, April 1998, paper # 98-2104.

[2]. Lou, M.C., Feria, V.A., and Huang, J., " Development of An Inflatable Space Synthetic Aperture Radar", proceedings of the 39th AIAA/ASME/ASCE/ AHS/ASC Structures, Structural Dynamics, and Materials Conference, Long Beach, CA, April 1998, paper # 98-2103.

[3]. Ruggiero, T.J., and Mikulas, M.M., " A One Dimensional Constitutive Model for wrinkled Thin Polymer Films", NASA Contractor Report # 201706, June 1997.

[4]. Van Wylen, G., Sonntag, R., and Borgnakke, C., Fundamentals of Classical Thermodynamics, John Wiley & Sons, Inc., 1994.

[5]. Perry, J.A., Jr., "Critical Flow Through Sharp Edged Orifices," Transactions of the American Society of Mechanical Engineers, October 1949, pp. 757-764.

[6]. Salama, M., Davis, G., Kuo, C.P., Rivellini, T., Sabahi, D., "Simulation of Airbag Impact Dynamics For Mars Landing", proceedings of the 37th AIAA Dynamics Specialists Conference, Salt Lake City, UT, April 1996, paper # 96-1209.

[7]. John Mc Kinney, and Tony Taylor, "Use of LS-DYNA3D to Simulate Airbag Landing Impact Attenuation of the Kistler K1 Reusable Launch Vehicle", 5th LS-DYNA Users Conference, Southfield, Mich., September 1998.

[8]. Hallquist, J.O., LS-DYNA3D, Theoretical / User's Manual, 1993.

[9]. Automatic Dynamic Analysis Mechanical Systems (ADAMS) / Solver Reference Manual, Version 9.1, 1998.

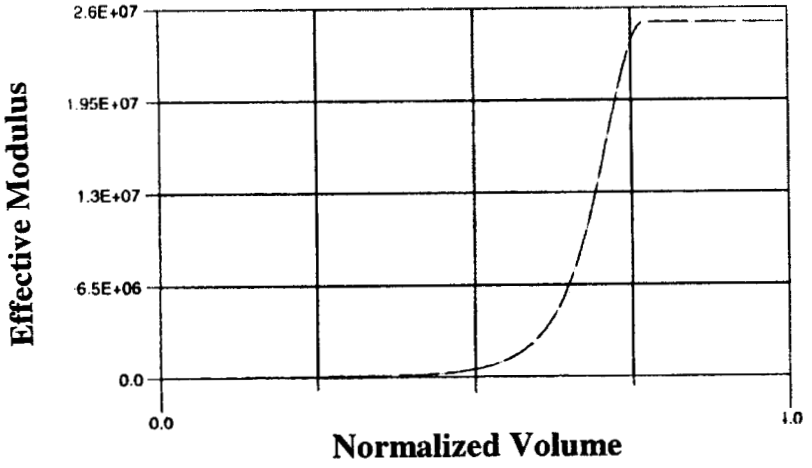

Figure (1): Constitutive Model of Wrinkled Membrane

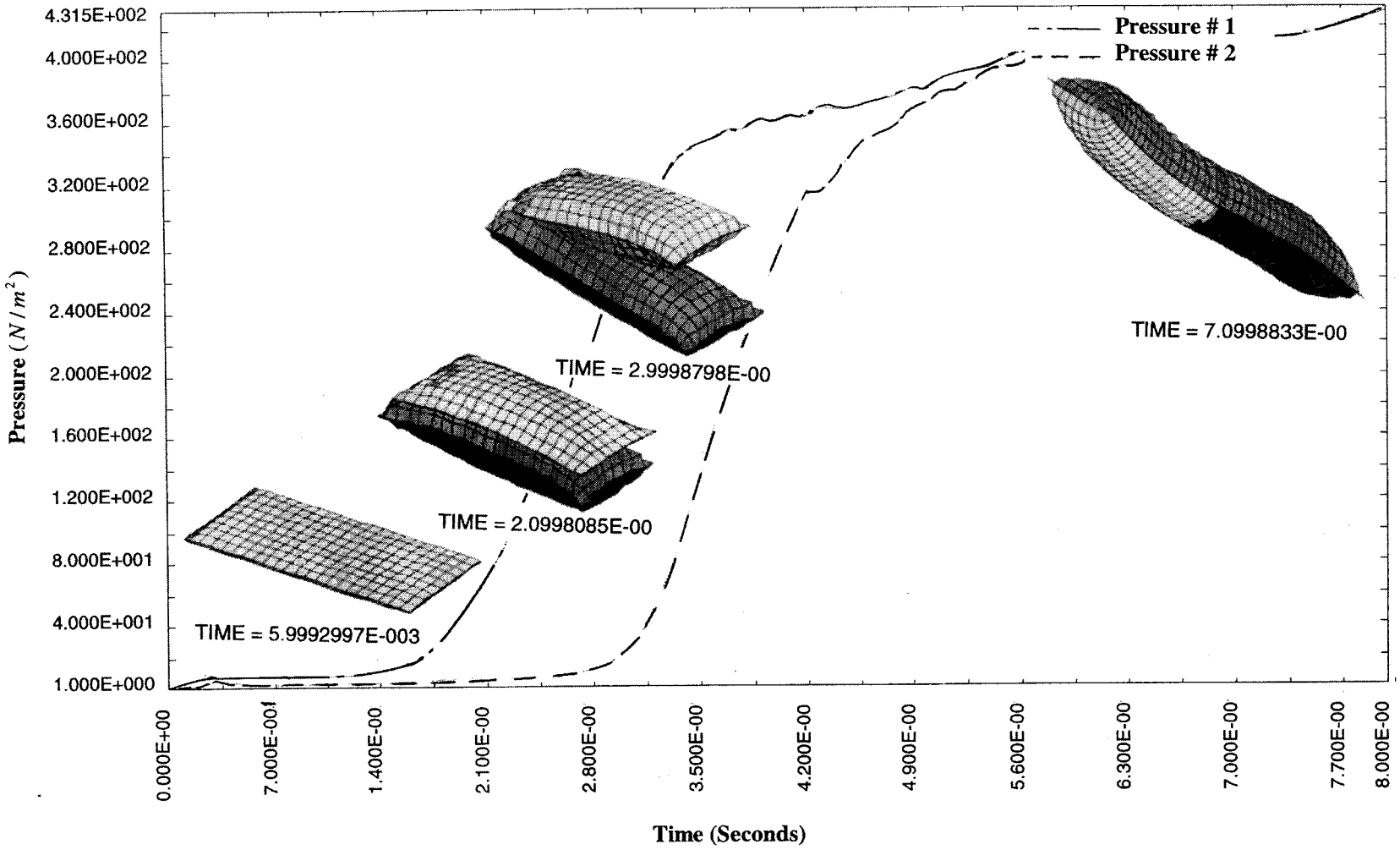

Figure (2): Deployment of a Z-Folded Tube

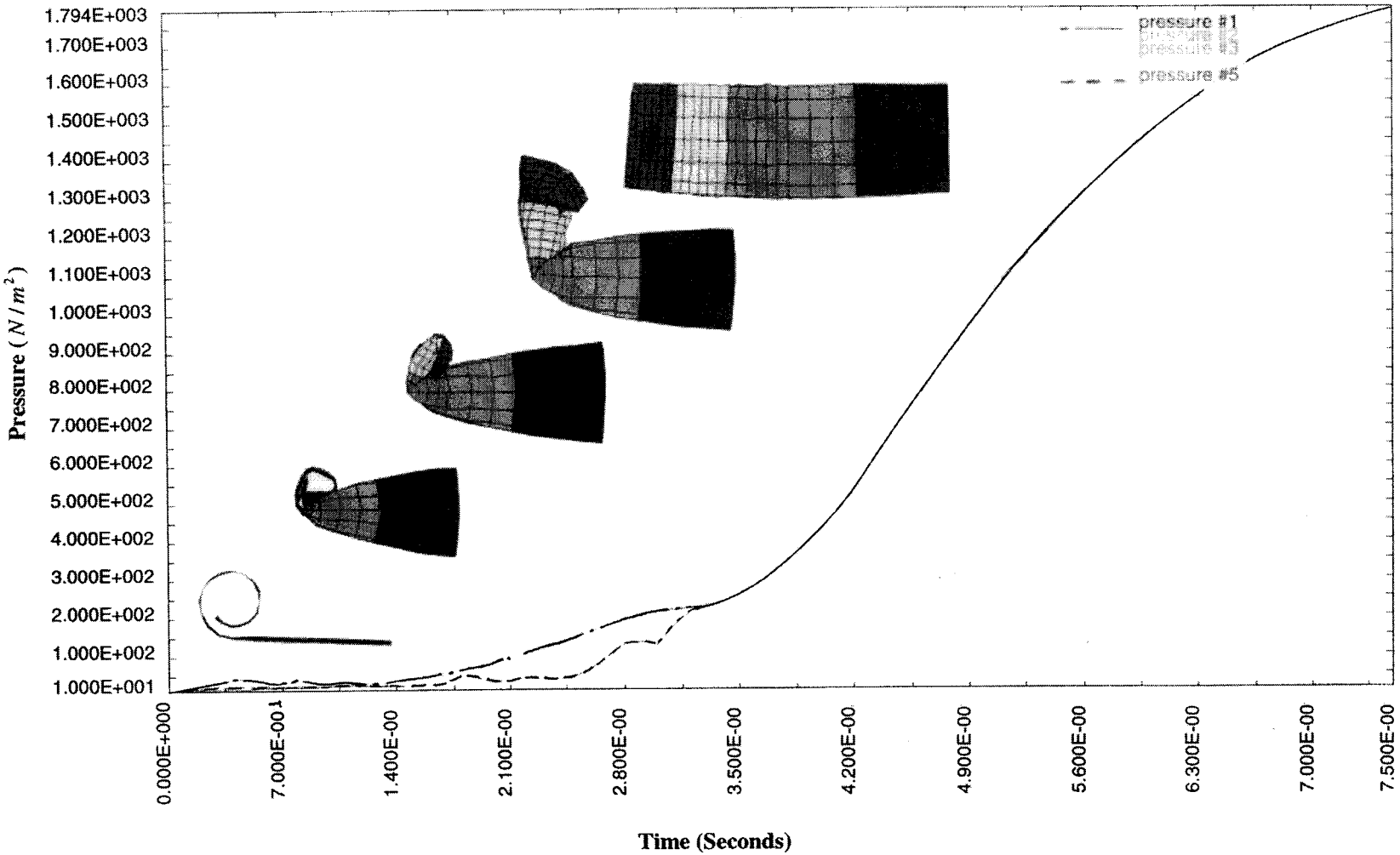

Figure (3): Deployment of a Rollout Tube

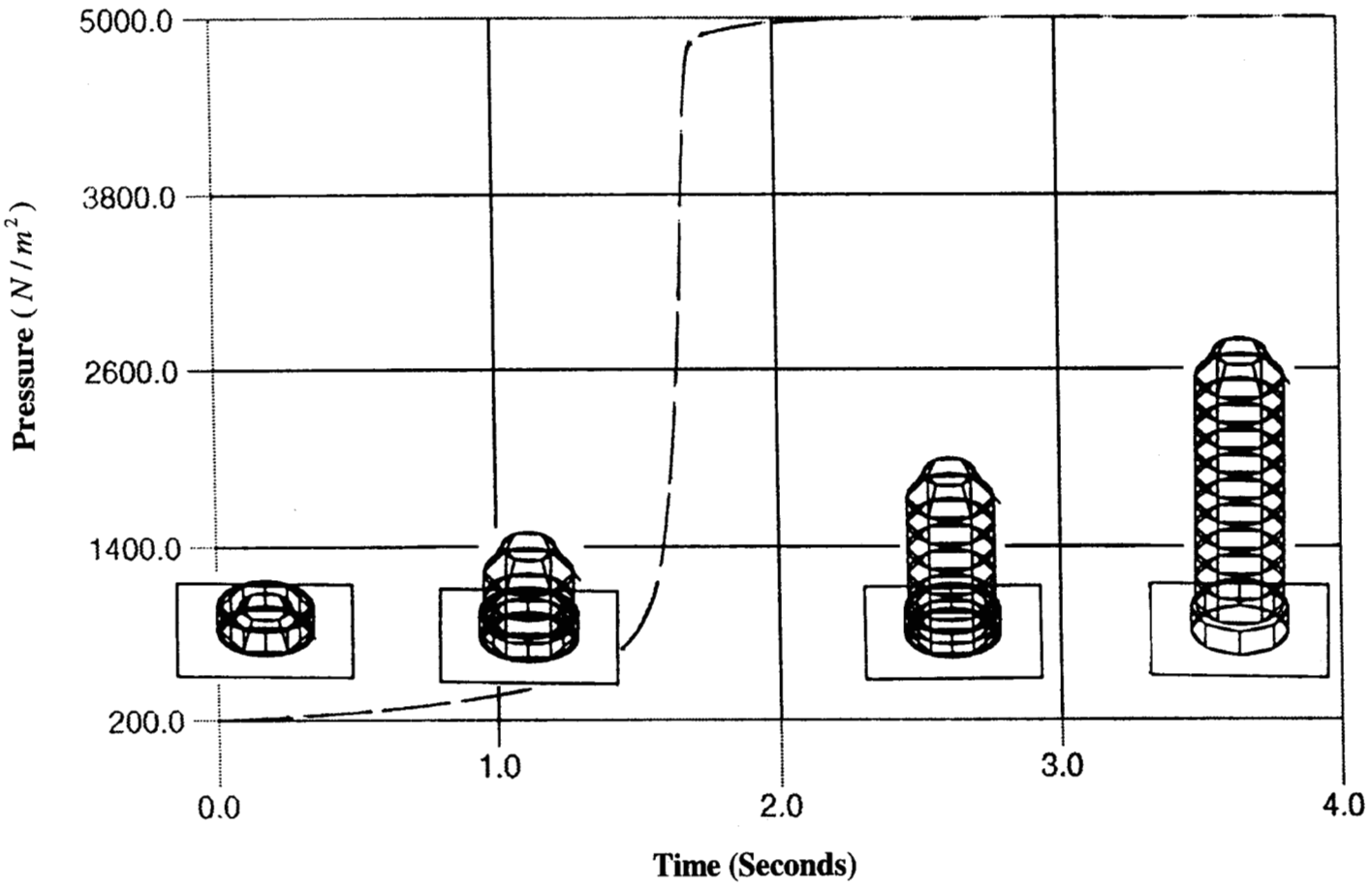

Figure (4): Deployment of Tube by Extrusion

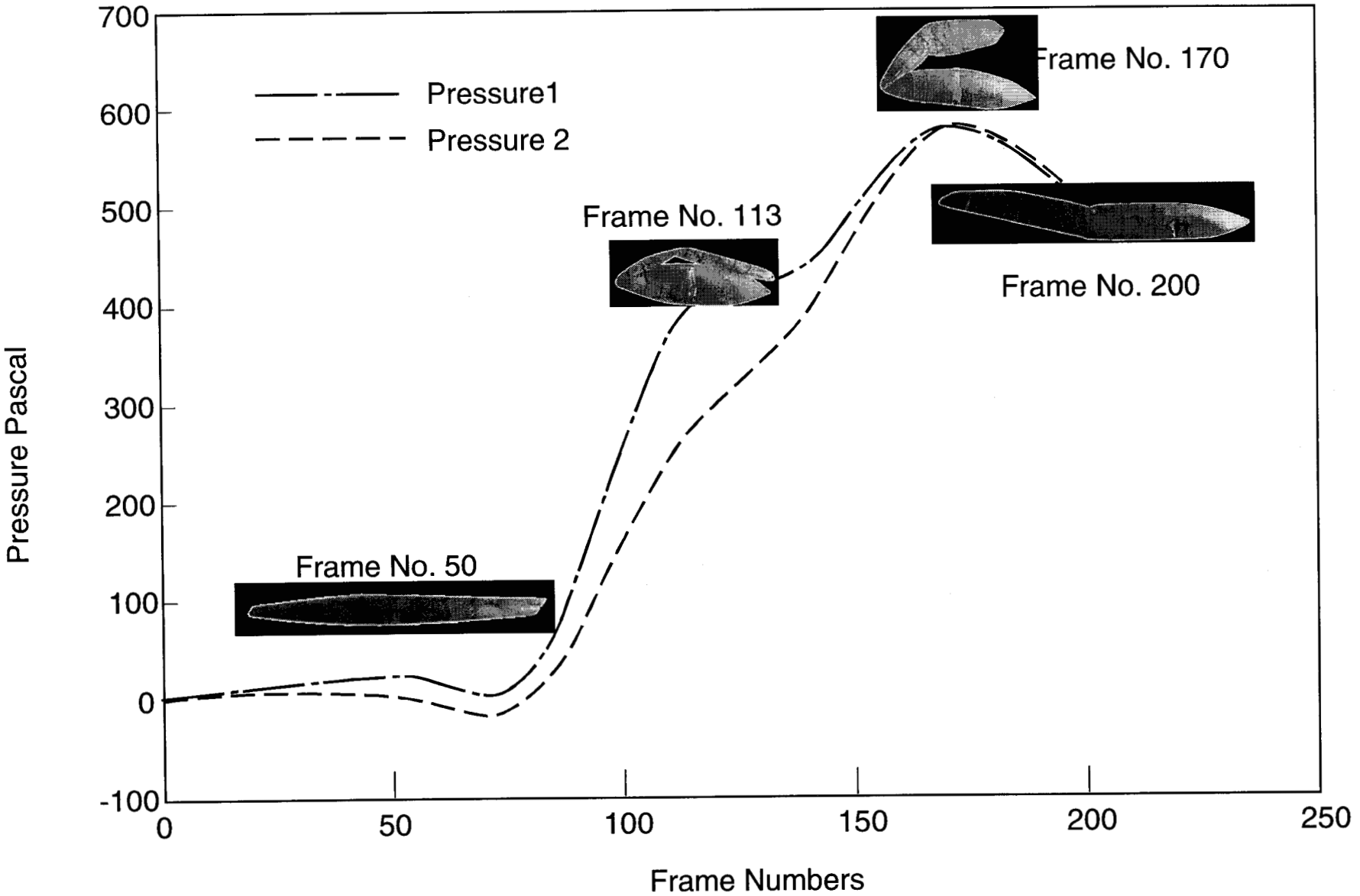

Figure (5): Experimental Deployment of a Z-Folded Tube